Synthesis, Biological Activity, and DNA-Damage Profile of Platinum−Threading Intercalator Conjugates Designed To Target Adenine

Rajsekhar Guddneppanavar,[†] Gilda Saluta,[‡] Gregory L. Kucera,[‡,§] and Ulrich Bierbach*,[†,§]

Department of Chemistry, Wake Forest University, Winston-Salem, North Carolina 27109, and Department of Internal Medicine, Hematology−Oncology Section, and Comprehensive Cancer Center of Wake Forest University, Wake Forest University School of Medicine, Winston-Salem, North Carolina 27157

PT-ACRAMTU {[PtCl(en)(ACRAMTU)](NO$_3$)$_2$, **2**; ACRAMTU = 1-[2-(acridin-9-ylamino)ethyl]-1,3-dimethylthiourea, **1**, en = ethane-1,2-diamine} is the prototype of a series of DNA-targeted adenine-affinic dual intercalating/platinating agents. Several novel 4,9-disubstituted acridines and the corresponding platinum−acridine conjugates were synthesized. The newly introduced 4-carboxamide side chains contain H-bond donor/acceptor functions designed to promote groove- and sequence-specific platinum binding. In HL-60 (leukemia) and H460 (lung) cancer cells, IC$_{50}$ values in the micromolar to millimolar range were observed. Several of the intercalators show enhanced cytotoxicity compared to prototype **1**, but conjugate **2** appears to be the most potent hybrid agent. Enzymatic digestion assays in conjunction with liquid chromatography−electrospray mass spectrometry analysis indicate that the new conjugates produce PT-ACRAMTU-type DNA damage. Platinum-modified 2′-deoxyguanosine, dG*, and several dinucleotide fragments, d(NpN)*, were detected. One of the conjugates showed significantly higher levels of binding to A-containing sites than conjugate **2** (35 ± 3% vs 24 ± 3%). Possible structure−activity relationships are discussed.

Introduction

The development of small molecules capable of interacting with nuclear DNA in a sequence- and groove-specific manner plays an important role in cancer chemotherapy.[1] As a consequence of our increased knowledge of the human genome and its roles in cell-signaling pathways, anticancer drug design is witnessing a paradigm shift away from chemically promiscuous electrophiles toward agents targetable to specific DNA-associated processes. Recent developments in the field of DNA-directed chemotherapy include agents that bind the promoter sequences of specific genes or sequences of specific nucleobase content, as well as molecules that target nonclassical DNA structures and DNA−enzyme complexes.[2,3] All of the above damage mechanisms interfere with the structural and functional integrity of the genome to alter or disrupt processes vital to cell-cycle progression, ultimately promoting cancer cell death.

Platinum drugs are among the most successful anticancer agents, and cisplatin [*cis*-diamminedichloroplatinum(II)] has become a mainstay in combination therapies, despite its serious clinical limitations.[4] Several of these limitations are thought to be linked to cisplatin's reactivity and lack of target specificity.[5] In a search for structurally novel non-cisplatin-type metallopharmacophores aimed at overcoming cisplatin's drawbacks, we have discovered a new class of platinum−intercalator conjugates that show promising in vitro activity at (sub)-micromolar concentrations in various solid tumors.[6−9] The prototype, PT-ACRAMTU (**2**, Figure 1), was generated by simple chemical linkage between the fragment [PtCl(en)]$^+$ (en = ethane-1,2-diamine) and the sulfur atom of the 9-aminoacridine derivative, 1-[2-(acridin-9-ylamino)ethyl]-1,3-dimethyl-
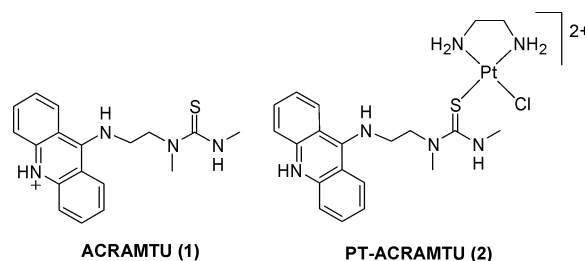

Figure 1. Structures of the drug prototypes.

thiourea (ACRAMTU (**1**), Figure 1). PT-ACRAMTU damages DNA by a dual mechanism involving intercalation and monofunctional platination, but it does not induce cross-links.[10] The hybrid agent produces adducts with guanine (G) and adenine (A), specifically in the sequences 5′-CG*A, 5′-CGA*, and 5′-TA*, where the asterisks denote the platinated bases.[11,12] This contrasts the DNA damage profile of cisplatin, which predominantly targets 5′-GG and 5′-AG base steps.[13] NMR studies indicate that the sequence and groove specificity of the ACRAMTU moiety is the source of the unique binding profile of PT-ACRAMTU.[14] In essence, the intercalator "hijacks" platinum away from G-N7 in the major groove, the thermodynamically and kinetically preferred binding site of divalent platinum, ultimately resulting in a DNA-damage profile complementary to that of the clinical drug. Most significantly, PT-ACRAMTU proves to be the first case of a platinum-based agent that targets the minor groove of B-form DNA. The distinct groove specificity of the 9-substituent in ACRAMTU leads to platination of A-N3 in the minor groove in ∼5−10% of the adducts.[15] Furthermore, we demonstrated using electrophoretic mobility shift assays (EMSA) that these adducts, when localized to 5′-TA sequences, inhibit the association of human TATA binding protein (hTBP) with its recognition sequence, a mechanism previously known for covalent and noncovalent intercalators and groove binders.[16] The potential biological implications of this type of damage are paramount: A-N3 adducts, if

* Address correspondence to this author. Telephone: 336-758-3507. Fax: 336-758-4656. E-mail: bierbau@wfu.edu.
† Department of Chemistry, Wake Forest University.
‡ Department of Internal Medicine, Wake Forest University School of Medicine.
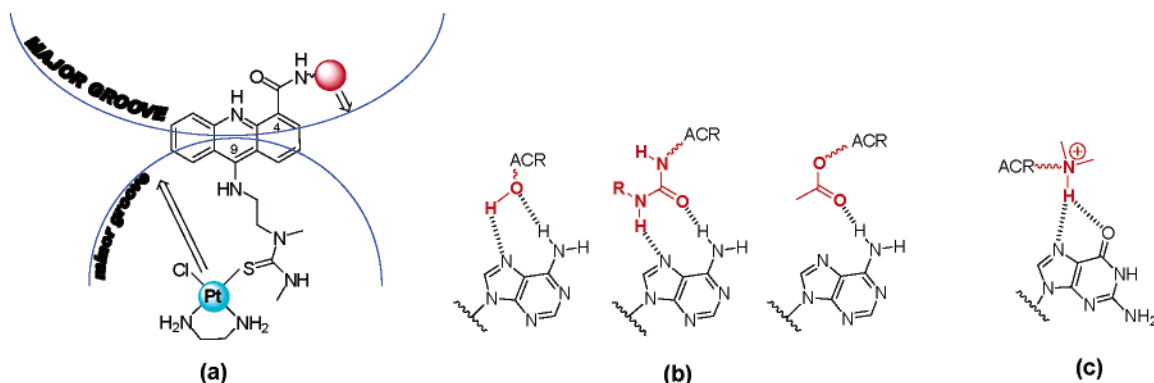§ Comprehensive Cancer Center of Wake Forest University, Wake Forest University School of Medicine.

Figure 2. Design rationale for novel 4,9-disubstituted ACRAMTU derivatives. (a) Regioselective threading intercalation and dual mechanism of groove recognition and platination (the red sphere represents a residue capable of H-bond formation, highlighted in red in b and c). (b) A-recognizing groups. (c) G-recognizing group.

frequently formed in genomic DNA, can be expected to contribute to the cytotoxic effect of PT-ACRAMTU by interfering with transcription initiation.[17]

As part of our efforts to delineate structure−activity relationships (SAR) within PT-ACRAMTU-type conjugates, we have now begun to extend our studies to analogues containing 4,9-disubstituted acridines derived from ACRAMTU. We hypothesize that modification of the planar chromophore with suitably functionalized side chains in the 4-position might provide a mechanism for tuning the sequence specificity of platination through additional noncovalent drug−nucleobase interactions in the DNA major groove. Here, we report the synthesis and biological activity of several of these "second-generation" ACRAMTU derivatives and their corresponding platinum conjugates. The DNA adduct profiles of the new conjugates were also studied using an enzymatic digestion assay in conjunction with in-line high-performance liquid chromatography−electropray mass spectrometry (LC−ESMS) analysis.

Results

Design. PT-ACRAMTU (**2**) induces damage at multiple nucleophilic sites in double-stranded DNA. Using a combination of enzymatic and newly developed acidic digestion assays we were able to demonstrate that in calf thymus DNA, for instance, complex **2** forms monoadducts with G (∼80%) and A (∼20%).[11] While N7 was the only targeted site in G, platination of A occurs at the N7 (∼11%), N3 (∼7%), and N1 (∼2%) positions.[15] All of these non-cisplatin-type adducts have to be considered potential cytotoxic lesions. (Reactions with native DNA were performed at drug-to-nucleotide incubation ratios (r_i) as high as 0.4.[15] It should be noted that while these conditions were appropriate for the detection and semipreparative chromatographic isolation of the major adducts, they may not reflect the true binding selectivity at physiological drug concentrations.) To investigate the inter-relationship between chemical structure, biological activity, and DNA damage profile, we are pursuing various strategies of modulating the nucleobase specificity of platination in PT-ACRAMTU-based conjugates. In particular, we are interested in chemical modifications of the prototype that might lead to enhanced targeting of adenine-containing sequences. The design applied in this study using threading intercalators can be rationalized as follows: Platination of nucleobase nitrogen occurs from a pre-intercalated state. The dynamic properties ("on/off" rates) and the base-pair-step and regiospecificity of this initial drug−DNA complex determine the base and site-selectivity of platinum binding. Of the two purine bases, G will be the preferred target in the major groove with Pt binding occurring at N7, whereas N3 of A can be

predicted to be the preferred binding site in the minor groove. Platination of minor-groove G-N3 should be disfavored due to the steric hindrance produced by the exocyclic $N(2)H_2$ group. Consequently, the targeting of the minor groove at A-containing base-pair steps can be expected to direct platinum away from its "natural" target, G-N7, and result in increased levels of A adducts.

The specific approach taken to tune the DNA binding of PT-ACRAMTU derivatives using 4,9-disubstituted acridines is summarized in Figure 2.

Groove Selectivity. In the proposed pre-intercalation complex the acridine chromophore is aligned with the base pairs' long dimensions at the intercalation pocket. In this geometry, the 9-substituent carrying platinum is directed toward the minor groove and the side chain in the 4-position protrudes into the major groove (Figure 2a), in accordance with the directionality of intercalation usually observed in the DNA complexes of acridine-based drugs, such as the acridine-4-carboxamides.[18,19] It is noteworthy to mention that ACRAMTU itself has been unequivocally demonstrated to intercalate DNA with the thiourea side chain residing in the *minor groove*.[14] (In a similar fashion, Denny et al. have synthesized major-groove and minor-groove targeted alkylating agents by tethering nitrogen mustard moieties to the 4- and 9-position of the acridine chromophore, respectively.[20,21])

Base Recognition. The design was inspired by the hydrogen-bonding interactions observed between purine bases and amino acid side chains in DNA−protein complexes. Crystal structures of proteins bound to the DNA major groove show that adenine has a high propensity for forming specific contacts with mixed donor−acceptor groups, such as the hydroxyl group in serine/threonine/tyrosine and the amide group in arginine/glutamine.[22] In contrast, hydrogen-bond donor groups, such as amine in lysine and guanidinium in asparagine, recognize guanine.[22] In this study, various functional groups were incorporated into the 4-carboxamide residues of the new ACRAMTU derivatives to mimic base-specific amino acid interactions with the ultimate goal of modulating the base selectivity of intercalation (and, ultimately, platination) via major-groove read-out by the drug molecule. Hydroxyl, urea, and methyl ester were chosen to specifically recognize A. A derivative containing a G-affinic dimethylammonium group was also included in the study (Figure 2b,c). There is precedent for the latter binding mode in the crystal structures of the DNA complexes formed by acridine-4-carboxamide anticancer agents (DACA), which preferentially intercalate into the 5′-CG/CG base-pair step.[18,19]

Molecular Modeling. To investigate the feasibility of the proposed mode of combined threading intercalation and major-

Scheme 1. Synthesis of Threading Intercalators and Platinum−Threading Intercalator Conjugates[a]
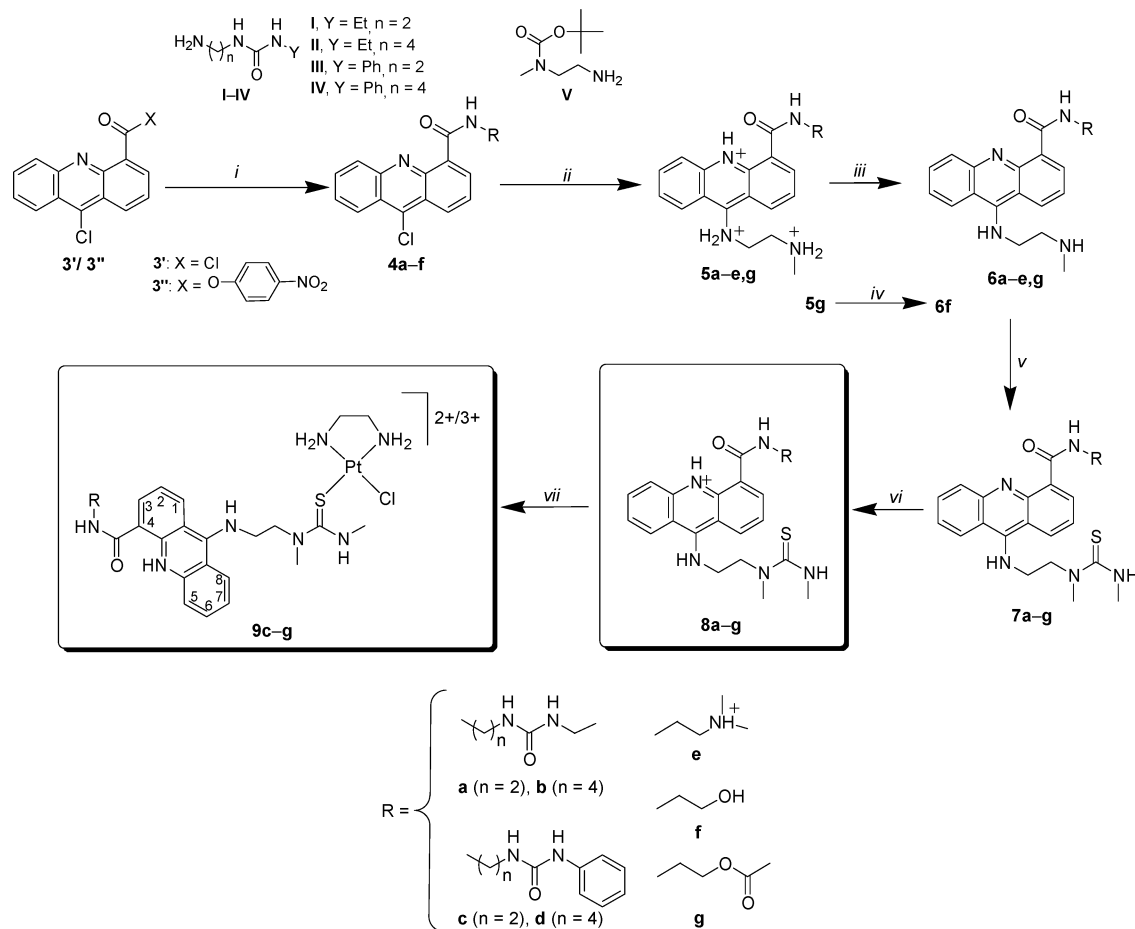
[a] Reagents and conditions: (i) **I−IV** (hydrochloride salts) or NH₂(CH₂)₂OH or NH₂(CH₂)₂N(CH₃)₂, Et₃N/CH₂Cl₂/0−5 °C; (ii) (1) phenol/**V**/Δ; (2) 2 M NaOH; (3) AcOH/HCl; (iii) 2 M NH₄OH; (iv) K₂CO₃/MeOH/H₂O; (v) CH₃NCS/EtOH/Δ; (vi) 1 M HNO₃; (vii) (1) [PtCl₂(en)], 1 equiv. AgNO₃/DMF/dark, rt; (2) **8c−g**, rt. The counterion in **5a−e, g** is Cl⁻, while the counterion in **8a−g** and **9c−g** is NO₃⁻.
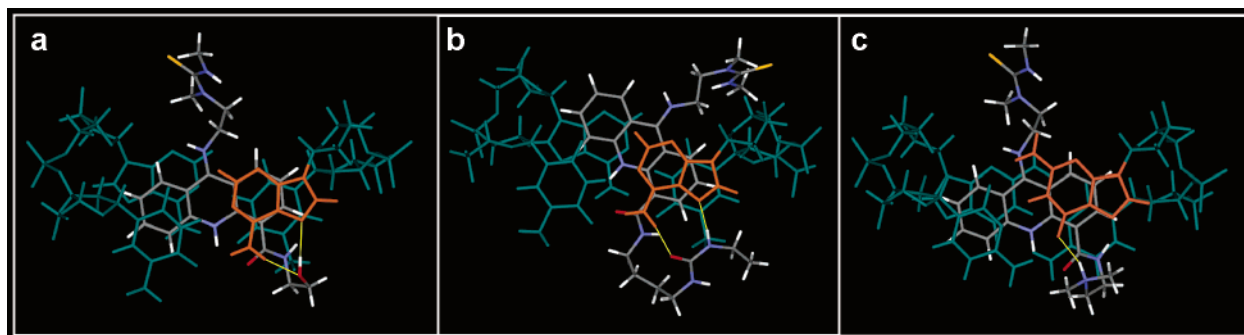

Figure 3. Views along the helical axis of AMBER-minimized models of duplexes containing threading intercalators. Only the intercalated drug molecules and the sandwiching base pairs (green) are shown. The nucleobase involved in hydrogen bonding with the drug molecule is highlighted in orange. The yellow solid lines indicate drug−DNA hydrogen bonding. (a) Derivative **8f** bound to the 5′-TA/TA step. Donor−acceptor distances: $O_{drug}\cdots N7_A$, 2.93 Å; $N6_A\cdots O_{drug}$, 3.03 Å. (b) Derivative **8b** bound to the 5′-TA/TA step. Donor−acceptor distances: $N6_A\cdots O_{drug}$, 2.95 Å; $N7_A\cdots N_{drug}$, 2.87 Å. (c) Derivative **8e** bound to the 5′-CG/CG step. Donor−acceptor distance: $N_{drug}\cdots O6_G$, 2.81 Å.

groove hydrogen bonding, molecular mechanics calculations were performed on DNA complexes containing several of the proposed ACRAMTU derivatives (for compound numbering used in this discussion, see Scheme 1). As starting structures, AMBER models of ACRAMTU bound to octamer duplexes previously derived from NMR data[14] were used. Specifically, intercalation of the hydroxyl- and urea-based derivatives (**8f** and **8b**) into the 5′-TA/TA base-pair step and a dimethylammonium-functionalized derivative (**8e**) into the 5′-CG/CG step was studied. During the early stages of the calculations the proposed hydrogen bonds were enforced by introducing suitable drug−

DNA distance constraints. After removal of the constraints, the freely minimized structures relaxed into the geometries shown in Figure 3. In all of the models, simultaneous threading intercalation and drug−nucleobase hydrogen bonding proves feasible without causing major conformational changes in the host duplex. Watson−Crick hydrogen bonding persists in the base pairs on both sides of the acridine chromophores. In all cases, the conformation of the 4-carboxamide side chains is stabilized by an intramolecular hydrogen bond between the amide oxygen and the protonated endocyclic acridine nitrogen (N10), a feature previously established for DNA-bound DACA-

type intercalators.[18,19] This arrangement positions the hydroxyl group in **8f** and the ammonium group in **8e** favorably for donor−acceptor interactions (Figure 3a,c) with minimal rearrangement of the chromophores relative to the geometry observed for ACRAMTU. This is in contrast to **8b**, whose planar unit has to twist significantly relative to the helical axis to allow dual hydrogen bonding between the urea group and adenine (Figure 3b; see figure caption for structural details). Another critical difference between the urea derivatives and **8e,f** is the requirement for an extended polymethylene chain. While an ethylene group produces the ideal geometry in **8e** and **8f**, a minimum of four carbon atoms are required to allow strainless hydrogen bonding of the urea moiety in **8b**.

Chemistry. The synthetic strategy for the preparation of the threading intercalators and the corresponding conjugates is outlined in Scheme 1. The first step involved reaction of the reactive 4-C(O)X group in 9-chloroacridine-4-carbonyl chloride (**3′**) or the analogous 9-chloro-*p*-nitrophenol ester (**3′**)[23] with the suitably functionalized primary amines to produce the 9-chloroacridine-4-carboxamide derivatives **4a−e** in 40−60% yield. Reactions performed with the *p*-nitrophenolato leaving group usually gave better yields (∼80% for **4f**). The urea-functionalized amines[24] **I−IV** were synthesized from the monoprotected 1,2- and 1,4-diamines by reaction of the unprotected amino group with ethyl isocyanate or phenyl isocyanate and isolated as the hydrochloride salts after removal of the BOC groups. Reaction of **4a−f** with (2-aminoethyl)-methylcarbamic acid *tert*-butyl ester (**V**) in the presence of excess phenol and base and subsequent deprotection of the secondary amino group resulted in intermediates **5a−e** and **5g** in form of their hydrochloride salts (35−45% yield for two steps). Under the esterifying conditions of the BOC group removal, **5g** is formed from **4f** rather than **5f**. The hydrochloride salts **5a−e** and **5g** were converted directly to the corresponding free bases, **6a−e** and **6g**, using dilute ammonium hydroxide solution, while hydrolysis of **5g** under strongly basic conditions afforded the desired 4-(2-hydroxyethyl)carboxamide derivative, **6f**. The secondary amino group in intermediates **6** was reacted with methylisothiocyanate to give the thioureas **7a−g**, which were converted to the corresponding hydronitrate salts **8a−g** (40−55% yield for two steps). Finally, the acridinium salts **8c−g** were reacted with the monoactivated form of [PtCl$_2$(en)], [PtCl-(DMF-*O*)(en)]$^+$, to generate the platinum−acridine conjugates **9c−g**.[9] Due to the high affinity of platinum for thiourea sulfur, a substantial amount of the corresponding platinum−bis-(acridine) complexes[25] were present in the reaction mixtures. Size-exclusion chromatography using nonaqueous eluents to avoid hydrolysis of the chloro ligands proved to be the only viable method for purifying several of the conjugates, which were obtained in 30−50% yield. Analogues **9a** and **9b** were not synthesized because of the marginal biological activity of the free acridine precursors (vide infra). The compounds included in the cell viability assays were fully characterized by ^{1}H and ^{13}C NMR spectroscopy, elemental analyses, and in-line LC−ESMS analysis (see Experimental Section and Supporting Information for details). The urea-based derivatives **8a−d** and **9c−d**, especially those containing extended linker chains (*n* = 4) in the 4-position, showed limited solubility in aqueous buffers compared to the prototypes **1** and **2** and derivatives **8/9e−g**.

Biological Activity. The new acridines and platinum−acridines along with the drug prototypes were tested in HL-60 leukemia and NCI-H460 lung cancer cell lines using a cell viability assay. The results are presented in Table 1. In the MTS-based colorimetric assay, the prototypical acridine derivative

Table 1. Cytotoxicity Data for **1**, **2**, **8a−g**, and **9c−g** (IC$_{50}$, μM)^a

acridines	HL-60^b	H460^b	platinum−acridines	HL-60	H460
1	11.5	9.5	**2**	2.8	0.26
8a	>100	>100	^{c}	—	—
8b	>100	>100	^{c}	—	—
8c	>50	31.9	**9c**	>50	26.7
8d	0.39	3.1	**9d**	1.5	3.7
8e	1.4	2.2	**9e**	10.6	6.1
8f	27.4	41.1	**9f**	39.7	3.8
8g	29.5	17.6	**9g**	30.2	8.4

^{a} MTS colorimetric cell proliferation assay; IC$_{50}$ values are given for 72-h drug exposure and are average values of at least three experiments. ^{b} HL-60, leukemia; H460, lung cancer. ^{c} Platinum conjugates of compounds **8a** and **8b** were not synthesized.

ACRAMTU (**1**) was moderately active in both cell lines. A significant enhancement in cytotoxicity is observed for PT-ACRAMTU (**2**), especially in the lung cancer line, where the conjugate is approximately 35-fold more active than the free acridine, a trend previously observed in clonogenic survival assays[9] performed with this cell line. The new derivatives **8a−g** show a broad range of activities with low micromolar to low millimolar IC$_{50}$ values. While analogues **8a−c**, **8f**, and **8g** show no cytotoxic response at drug concentrations as high as 100 μM or prove to be significantly less active than **1**, compounds **8d** and **8e** are more active than the prototype. In particular, derivative **8d** showed a cytotoxic effect in HL-60 cells in the low micromolar range (IC$_{50}$ = 0.39 μM), previously observed only for platinum conjugates such as **2** and a few of its direct derivatives. Two interesting effects are observed within the subgroup of urea analogues, **8a−d**, where both the presence of an *n* = 4 and a phenyl group on the terminal urea nitrogen seem to be a prerequisite for appreciable cytotoxicity. Characteristically, both extension of the 4-carboxamide side chain in **8c** by two carbon atoms and replacement of the ethyl with the phenyl group in derivative **8b** to yield compound **8d** lead to a dramatic increase in cytotoxicity by >100-fold on the basis of the inhibitory concentrations determined in both cell lines. From the molecular modeling study it seems plausible that the inferior activity of the more constrained derivatives, **8a** and **8c**, may be a consequence of their inability to form stable drug−DNA complexes via threading intercalation. It is unclear what causes the increase in activity by the simple ethyl/phenyl substitution. In the platinum conjugates **9c** and **9d**, an increase in potency is observed with an increase in 4-carboxamide chain length, in agreement with the trend observed for the corresponding free acridines. The majority of the conjugates generated, however, show activity similar to that established for the platinum-free intercalators. A significant effect of the metal on cytotoxicity levels comparable to that established for the prototypical complex is observed for conjugate **9f**; however, only the H460 cell line appears to be sensitive to this type of structural modification.

DNA Damage. To gain insight into the effects of the structural modifications on the DNA-damage profiles of the newly synthesized conjugates, enzymatic digests of native DNA treated with selected derivatives were qualitatively and quantitatively analyzed by in-line LC−ESMS using an experimental setup described previously.[11] Briefly, calf thymus DNA was incubated with **2** and **9d−f**, unbound drug removed from the reaction mixtures by microdialysis, and the platinated DNA samples enzymatically digested and dephosphorylated using an approved "cocktail" of endonucleases and alkaline phosphatase. The adducts were then separated by reverse-phase chromatography and identified by ESMS run in negative ion mode. In all

Table 2. Summary of Platinum−Acridine-Modified DNA Fragments Observed in Enzymatic Digests

conjugates	fragments	molecular ion	% abundance	m/z
2	dG* [a]	$[M - 4H]^-$	66(8)	843.3
	(GpA/ApG)*	$[M - 3H]^-$	13(2)	1156.3
	(TpG/GpT)*	$[M - 3H]^-$	10(3)	1147.3
	(TpA/ApT)*	$[M - 3H]^-$	7(2)	1131.3
	(ApA)*	$[M - 3H]^-$	4(2)	1140.3
9d	dG*	$[M - 4H]^-$	45(4)	1076.5
	(GpA/ApG)*	$[M - 3H]^-$	15(1)	1389.6
	(TpG/GpT)*	$[M - 3H]^-$	13(0)	1380.5
	(TpA/ApT)*	$[M - 3H]^-$	11(1)	1364.6
	(ApA)*	$[M - 3H]^-$	9(3)	1373.5
	(GpG)*	$[M - 3H]^-$	7(0)	1405.5
9e	dG*	$[M - 5H]^-$	46(12)	957.4
	(GpA/ApG)*	$[M - 4H]^-$	13(4)	1270.5
	(TpG/GpT)*	$[M - 4H]^-$	32(2)	1261.5
	(TpA/ApT)*	$[M - 4H]^-$	9(1)	1245.5
9f	dG*	$[M - 4H]^-$	58(8)	930.4
	(GpA/ApG)*	$[M - 3H]^-$	17(2)	1243.5
	(TpG/GpT)*	$[M - 3H]^-$	11(2)	1234.6
	(TpA/ApT)*	$[M - 3H]^-$	8(1)	1218.4
	(ApA)*	$[M - 3H]^-$	3(1)	1227.7
	(GpG)*	$[M - 3H]^-$	3(0)	1259.4

[a] The asterisks denote the moieties $[Pt(en)(\mathbf{1/8d-f})]^{3+/4+}$.

the cases, enzymatic degradation of the drug-treated DNA resulted in platinum-modified guanosine and multiple dinucleo-

tide fragments, but no (undigested) trinucleotides and higher modified oligonucleotides were detected in the mixtures. The results of this assay are summarized in Table 2 and Figure 4. Previously, three adducts of conjugate **2** were detected: dG* (dG = 2′-deoxyguanosine), 5′-GpA*, and 5′-TpA*, where the asterisk represents the platinum−acridine fragment [Pt(en)-(**1**)]$^{3+}$.[11] The sequence specificity (e.g., 5′-TpA* vs 5′-A*pT) and base specificity (e. g., in the 5′-GpA sequence) of the damage in the latter dinucleotide fragments could be fortuitously determined from tandem MS data,[11] which were confirmed by high-resolution structural and footprinting techniques.[12,15,26] While the data acquired in the present study did not provide this structural detail, the nucleobase content of the modified dinucleotide fragments could be unambiguously established on the basis of their expected molecular ions, $[M - nH]^-$, observed in negative ion mode mass spectra (Table 2; for HPLC traces and mass spectra, see Supporting Information). The current study confirms the DNA damage produced by conjugate **2**. In addition to the three modified fragments detected in previous assays, two new dinucleotide adducts are observed, (TpG/GpT)* (9%) and (ApA)* (4%). While the former damage site is quite unexpected, the latter minor adduct confirms the damage within
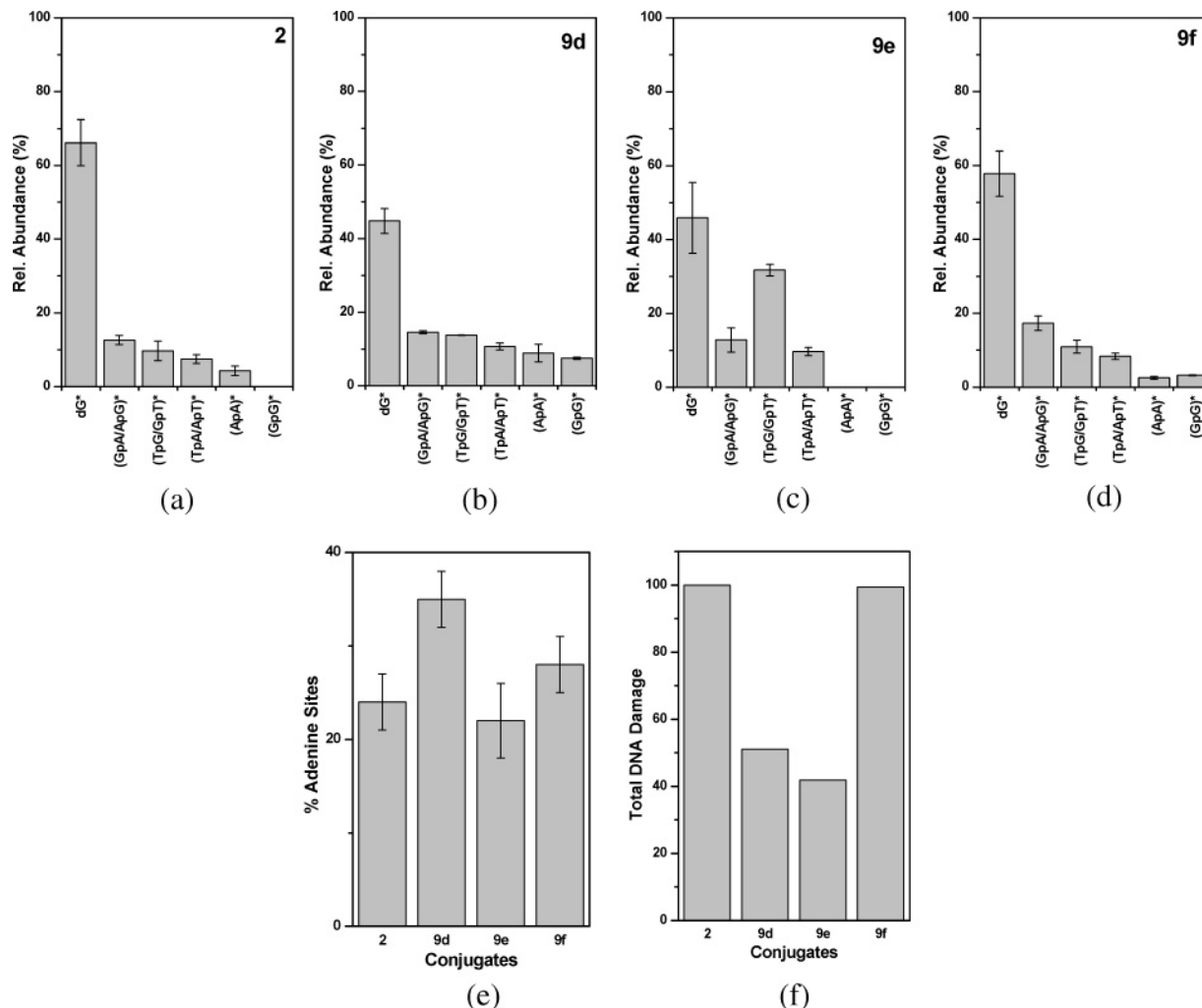

Figure 4. (a−d) Relative abundance of platinum−acridine-modified DNA fragments observed in enzymatic digests of calf thymus DNA treated with conjugates **2** and **9d−f**. Drug-modified mononucleoside and dinucleotide fragments were separated and characterized by in-line LC−ESMS. Relative abundances were determined by integrating the intensities of HPLC peaks monitored at acridine-specific wavelengths using diode-array detection. Plotted values are the average of three individual incubations/digestions, and error bars represent ±1 standard deviation. Assignments for dinucleotide fragments are non-sequence- and non-base-specific. The notation (GpA/ApG)*, for instance, indicates a fragment in which either G or A is platinated. The asterisks represent the platinum moieties [Pt(en)(**1/8d−f**)]$^{3+/4+}$. (e) Percent targeted A-containing dinucleotide sites by each drug. (f) Plot of relative total degree of modification by each drug (prototype **2** = 100), based on all platinum-containing fragments.
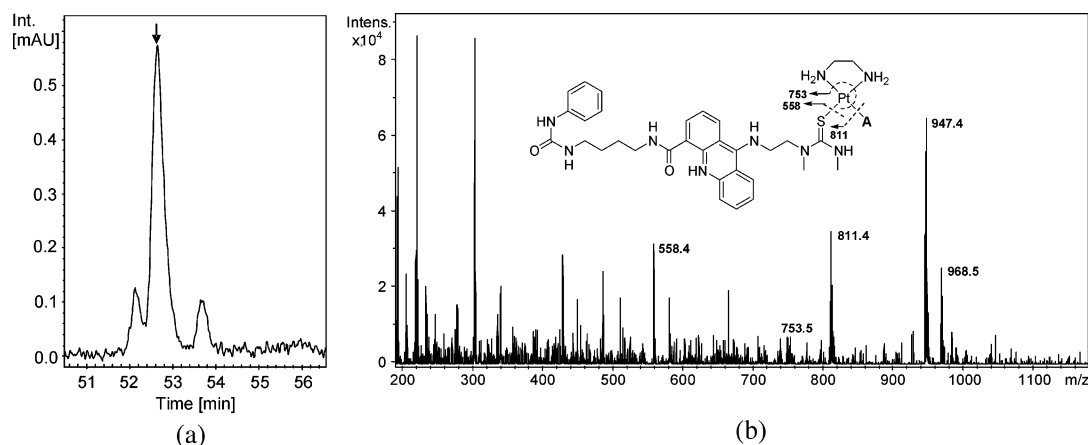
Figure 5. (a) Reverse-phase HPLC profile monitored at 414−430 nm of an acidic digest of a double-stranded decamer treated with conjugate **9d**. The arrow indicates the major drug-modified fragment, which elutes at a retention time of 52.7 min. (b) Positive-ion electrospray mass spectrum of the major adduct. The inset shows the structure of the adduct and fragments resulting from CAD. "A" stands for adenine nucleobase.

the sequence 5′-TAA detected by transcriptional footprinting.[12] In this sequence a stop site was observed at the 3′-A base, suggesting platination of this nucleobase and intercalation of the acridine chromophore between the purine bases, which apparently protects the phosphodiester linkage in the ApA sequence from enzymatic cleavage. (This mode of sequence-specific intercalation has been discussed to explain the previously detected modified fragments.[11]) In 24% of the adducts identified, prototype **2** targets A-containing dinucleotide steps. Upon first inspection, the type of damage induced by conjugates **9d**−**f** is similar to that of **2** based on the fragments identified (Figure 4b−d). In the case of **9d** and **9f**, a small amount of undigested (GpG)* is observed with abundances of 7% and 3%, respectively, and the adduct distribution differs significantly from that of the parent complex. Most significantly, the amount of dG* is notably reduced. This effect is most pronounced for **9d** and **9e**, for which this species accounts for 45% and 46% of the total array of adducts, respectively. In the case of **9d**, a significant increase in modified A-containing fragments is observed relative to complex **2**, accounting for 35% of the total adducts. In contrast, conjugate **9e** containing the G-directed dimethylaminoethyl residue shows the lowest affinity for A (22% of adducts; Figure 4e) but, curiously, produces a large amount of (TpG/GpT)* (32% of adducts). In **9e**, simultaneous platination of G-N7 and H-bond formation by the NHMe$_2$ group with the same G in the major groove are incompatible. Thus, it may be speculated that in the TpG/GpT sequence platination of G occurs at N3 in the minor groove. Additional analytical and high-resolution structural work, however, is required to explore this possibility. Complex **9f** shows an adduct profile qualitatively and quantitatively similar to that of **2**. Finally, the overall DNA binding levels produced by derivatives **9d** and **9e** are significantly reduced compared to those observed for analogues **2** and **9f**, based on the total amount of adducts detected for each agent (Figure 4f).

While the results of the enzymatic digestion convincingly demonstrated that all of the new conjugates target A-containing sites, this assay did not provide direct evidence for coordinative attachment of platinum to A in the dinucleotide fragments isolated, such as (TpA/ApT)* and (GpA/ApG)*. To demonstrate that A residues are platinated, a previously designed depurination assay[15] was employed. The assay takes advantage of the fact that platinum-modified A can be easily liberated from drug-treated DNA samples under mildly acidic conditions. In this experiment, conjugate **9d**, the derivative exhibiting the highest affinity for A-containing sequences (see Figure 4e), was

incubated at limiting concentrations of drug with the model duplex d(GCGATATCGC)$_2$, which contains several of the predicted high-affinity sites of this agent. The modified sequence was then digested at 60 °C/pH 2 and the mixture analyzed by LC−ESMS as described previously. The major adduct observed in the HPLC traces (Figure 5a) was indeed identified as the monofunctional A adduct [Pt(en)(**8d**)(A)]$^{3+}$ ([M]$^{3+}$). Electrospray mass spectra of this fraction acquired in positive-ion mode in conjunction with fragmentation by in-source collisionally activated dissociation (CAD) (Figure 5b) was used to establish the nature of this species. Two peaks are observed for the intact adduct, [M − 2H]$^+$ (947 m/z) and [M − 3H,Na$^+$]$^+$ (968 m/z). Fragment ions are also observed resulting from loss of A base, [M − A − 2H]$^+$ (811 m/z), and loss of both A and en ligand, [M − A − en − 2H]$^+$ (753 m/z). All of these ions show the characteristic isotope pattern of platinum. In addition, a peak is observed at 558 m/z, which is assigned to the protonated free acridine, [**8d**]$^+$, resulting from dissociation of the Pt−S bond in conjugate **9d**. On the basis of the ESMS data, it is not possible to discern the platinated nitrogen in A (N1, N3, or N7).

Discussion

The major goal of this study was to examine the possibility of tuning the DNA interactions of a novel platinum−acridinylthiourea pharmacophore through chemical modification of the drug prototype, PT-ACRAMTU (**2**). The targeting of DNA-binding molecules to A-rich sequences of the genome that are critical to cell function, such as TATA-based gene promoters[27−30] and AT-islands,[31] is an unexplored opportunity in platinum antitumor chemistry. The divalent metal has a high binding preference for G, and the N7 position of this base in the major groove is the primary binding site of virtually all platinum-based drugs in clinical use or clinical trials.[32] Inspired by the discovery of conjugate **2**, which breaks this long-standing paradigm by producing a high percentage of monofunctional A adducts, structural changes were made to the prototype that would result in more selective binding to A-containing sequences. The strategy employed here is based on the supposition that the sites of irreversible platinum damage can be controlled by the sequence and groove specificity of the threading intercalators. While this binding mode is unknown in platinum−DNA chemistry, several examples exist of bioactive intercalator−alkylator conjugates that act through this mechanism: the pluramycins[33−37] and psorospermins[38,39] are cytotoxic compounds in preclinical development that intercalate double-

stranded DNA sequence- and groove-specifically to produce epoxide-mediated covalent adducts with G-N7 in the major groove.

While the bioanalytical data suggest that the DNA-damage profile of the new conjugates is altered compared to that of complex **2**, at least for one of the derivatives synthesized, **9d**, more drastic modifications seem to be necessary to produce a truly A- and minor groove-specific platinum agent. Given the distinct G-N7 specificity of this metal, this is not a trivial task. Characteristically, previous attempts to direct platinum into the minor groove by tethering the metal to distamycin were unsuccessful.[40,41] This contrasts the situation for minor-groove alkylation, which can be readily induced by tethering an appropriate electrophile to a minor-groove-specific agent. 9-Anilinoacridine−nitrogen mustard conjugates[20,42] and *N*-methylpyrrolecarboxamide dipeptide modified with a methyl sulfonate ester ("Me−lex")[43] are examples of agents that have been successfully designed to produce covalent adducts in the minor groove, especially with A-N3. In the case of PT-ACRAMTU-type conjugates, a combination of (threading) intercalation and more efficient sequence recognition in the minor groove by polyamide-type structures might provide a means of producing less promiscuous agents with more predictable groove and long-range sequence specificity. These studies are currently underway.

Several interesting structure−activity relationships are observed in compounds **8a−d**, but no direct relationship seems to exist between the absolute cytotoxicity levels and the DNA damage produced by the conjugates. Compounds **2** and **9f** show similar adduct profiles (Figure 4a,d) and overall levels of platinum adducts (Figure 4f). Among the conjugates tested, the two derivatives show the most pronounced differential inhibitory effects in HL-60 and H460 cells: both compounds are ∼10-fold more active in the solid tumor cell line compared to the leukemia cell line. In addition, **2** and **9f** show greatly enhanced activity compared to the free acridines in H460 cells, suggesting that both compounds may act by a common mechanism in this cell line. In contrast, no metal-enhanced activity is observed for **9c−e**. This raises the question as to the role of platinum in the mechanism of DNA damage. Clearly, the hybrid binding mode involving monofunctional platination differs from cis-platin-induced cross-links. The 1,2 intrastrand cross-link, cis-platin's major adduct, bends DNA significantly, a structural distortion that is thought to trigger cell death mediated by high-mobility group (HMG) proteins, which tightly associate with this lesion.[44−46] The NMR solution structure of the monofunctional G adduct formed by **2** suggests that the combination of platination and intercalation significantly unwinds DNA locally but does not bend the duplex.[26] It is possible that platinum in our hybrid agents primarily acts as a "covalent anchor" that turns reversible intercalation into permanent damage and, ultimately, prevents dissociation of the acridine derivative from DNA. Because long-lived (here, irreversible) intercalator−DNA complexes often interfere with RNA polymerases to disrupt transcription,[47] platinum might turn the acridines into more efficient transcription inhibitors. This would explain why modification with platinum of ACRAMTU (**1**), the simplest acridine derivative in the series, whose DNA binding is characterized by rapid on/off rates,[14] results in greatly enhanced cytotoxicity levels. On the other hand, platinum in conjugate **9d**, for instance, containing a potentially threading intercalator that can be expected to form longer-lived intercalative complexes with DNA, apparently does not contribute at all to the cytotoxicity of the conjugate (see Table 1 for a comparison of

IC_{50} data determined for **8d** and **9d** in the H460 cell line). In summary, while there appear to exist no obvious correlations between DNA-damage profile and biological activity, several interesting structure−activity relationships are observed that may prove useful in our continued search for the DNA-processing enzymes involved in the mechanism of these novel hybrid agents. In particular, the ultimate role of transcription inhibition in the mechanism of these conjugates has yet to be established. Furthermore, it will be of interest to assess if the new hybrid agents might act through a topoisomerase-dependent mechanism similar to the mixed alkylating−intercalating psorospermin.[38,39] In addition to the differences in the DNA-damage profiles, other factors may exist, such as differential drug uptake and efflux, which may limit the cytotoxic effect of the conjugates. Future studies will address these issues.

Experimental Section

Synthetic Chemistry and Product Characterization. ^{1}H NMR spectra for the target compounds and intermediates were recorded on Bruker Avance 300 and DRX-500 instruments operating at 500 and 300 MHz, respectively. ^{13}C NMR spectra were recorded on a Bruker Avance 300 instrument operating at 75.5 MHz. Chemical shifts (δ) are given in parts per million (ppm) relative to internal standard trimethylsilane (TMS) or 3-(trimethylsilyl)-1-propane-sulfonic acid sodium salt (DSS) for samples in D_2O. Coupling constants (J) are in Hz. [1]H chemical shift assignments for the target compounds **8a−f** and **9c−f** were assisted by gradient COSY and ^{1}H-detected gradient HSQC and HMBC spectra recorded on a Bruker DRX-500 MHz spectrometer. Elemental analyses were performed by Quantitative Technologies Inc., Madison, NJ. All reagents were used as obtained from commercial sources without further purification unless indicated otherwise. Solvents were dried and distilled prior to use. Sephadex LH-20 resin was purchased from Amersham Biosciences. The HPLC/MS data of compounds **8a** and **9c−f** were collected on an Agilent Technologies 1100LS/MSD Trap instrument equipped with an atmospheric pressure electrospray ionization system and a multiwavelength diode array detector.

The following compounds were prepared according to previously described procedures: 1-[2-(acridin-9-ylamino)ethyl]-1,3-dimeth-ylthiourea HNO_3 salt (ACRAMTU, **1**), [PtCl(en)(ACRAMTU)]-$(NO_3)_2$ (PT-ACRAMTU, **2**), and (2-aminoethyl)methylcarbamic acid *tert*-butyl ester (**V**),[9] and 9-chloroacridine-4-carbonyl chloride (**3′**), 9-chloroacridine-4-carboxylic acid 4-nitrophenyl ester (**3″**), and 9-chloroacridine-4-carboxylic acid (2-dimethylaminoethyl)amide (**4e**).[23]

Synthesis of Urea Derivatives I−IV. All compounds were synthesized according to a procedure reported previously for *N*-(2-aminoethyl)-*N′*-phenylurea (**III**)[24] and isolated as hydrochloride salts.

1-(2-Aminoethyl)-3-ethylurea Hydrochloride, I. ^{1}H NMR (D_2O): δ 3.41 (2H, t, $J = 5.8$), 3.14−3.07 (4H, m), 1.07 (3H, t, $J = 7.2$).

1-(4-Aminobutyl)-3-ethylurea Hydrochloride, II. ^{1}H NMR (DMSO-d_6): δ 8.08 (br s), 6.78 (br s), 3.04−2.97 (4H, m), 2.80−2.69 (2H, m), 1.44−1.35 (2H, m), 1.59−1.49 (2H, m), 0.98 (3H, t, $J = 7.2$).

1-(4-Aminobutyl)-3-phenylurea Hydrochloride, IV. ^{1}H NMR (DMSO-d_6): δ 8.73 (1H, br s), 7.84 (2H, br s), 7.38 (2H, d, $J = 8.1$), 7.20 (2H, t, $J = 7.9$), 6.88 (1H, t, $J = 7.2$), 3.09 (2H, $J = 6.4$), 2.85−2.74 (2H, m), 1.62−1.44 (4H, m).

Compounds **4a−d** were synthesized using a common procedure. A typical synthetic procedure is described for **4c** below.

9-Chloroacridine-4-carboxylic Acid [2-(3-Phenylureido)ethyl]-amide, 4c. A mixture of 4.296 g (19.92 mmol) of 1-(2-aminoethyl)-3-phenylurea hydrochloride (**III**) and 15.14 mL (108.7 mmol) of triethylamine in anhydrous CH_2Cl_2 (50 mL) was stirred for 1 h at room temperature. The reaction mixture was cooled to 0 °C and 5.0 g (18 mmol) of 9-chloroacridine-4-carbonyl chloride (**3′**) was

added in one portion. The reaction mixture was stirred for another 4−5 h and then evaporated to dryness. The residue was washed thoroughly with water and redissolved in $CHCl_3$. The solution was dried with anhydrous Na_2SO_4, filtered, and evaporated to dryness. The reddish oil obtained was treated with diethyl ether to yield **4c** as a yellow microcrystalline solid (yield 4.0 g, 53%). ^{1}H NMR (DMSO-d_6): δ 11.18 (1H, br s), 8.78 (1H, d, *J* = 7.0), 8.66 (1H, s), 8.62 (1H, d, *J* = 8.6), 8.44−8.36 (2H, m), 7.89 (1H, t, *J* = 7.8), 7.83−7.79 (2H, m), 7.39 (2H, d, *J* = 7.7), 7.19 (2H, t, *J* = 7.8), 6.88 (1H, t, *J* = 7.3), 6.44 (1H, br s), 3.72−3.66 (2H, m), 3.54−3.48 (2H, m).

9-Chloroacridine-4-carboxylic Acid (2-Hydroxyethyl)amide, 4f. Compound **3″** (7.5 g, 19.8 mmol) was added to an ice-cooled stirred solution of 2-aminoethanol (1.36 mL, 22.5 mmol) and triethylamine (6.27 mL, 45.0 mmol) in anhydrous CH_2Cl_2 (50 mL). After stirring at 0−5 °C for 4 h, the solvent was evaporated, and the residue was washed thoroughly with cold absolute ethanol, filtered, and dried in a vacuum, giving **4f** as a yellow powder (4.646 g, 78%), which was used in the next step without further purification. ^{1}H NMR (DMSO-d_6): δ 11.50 (1H, br s), 8.79 (1H, dd, *J* = 7.1, 1.3), 8.60 (1H, dd, *J* = 8.7, 1.3), 8.43 (1H, d, *J* = 8.6), 8.31 (1H, d, *J* = 8.7), 8.05 (1H, t, *J* = 7.7), 7.91−7.83 (2H, m), 5.07 (1H, br s), 3.78−3.72 (2H, m), 3.65−3.60 (2H, m).

Compounds **5a−e** and **5g** were synthesized from **4a−e** and **4f**, respectively, using a common procedure. A typical procedure is described below for **5c**.

9-(2-Methylaminoethylamino)acridine-4-carboxylic Acid [2-(3-Phenylureido)ethyl]amide Trihydrochloride, 5c. A mixture of **4c** (4.0 g, 9.55 mmol) and dry phenol (8.98 g, 95.5 mmol) was heated at 60 °C for 30 min. To the clear solution, (2-aminoethyl)-methylcarbamic acid *tert*-butyl ester (**V**) (1.90 g, 10.9 mmol) was added in one portion, and stirring was continued at 120 °C for 2 h. The reaction mixture was cooled to room temperature and poured into 400 mL of 2 M NaOH solution. The mixture was extracted with $CHCl_3$, and the organic layer was dried over anhydrous Na_2SO_4, filtered, and evaporated to dryness to afford a bright orange viscous oil. The residue was dissolved in a mixture of CH_3COOH (100 mL) and concentrated HCl (10 mL) and stirred at room temperature for 1.5 h. After removal of the acid using a rotary evaporator, the resulting reddish oil was treated with a 1:1 mixture of ethanol and diethyl ether to crystallize compound **5c** (2.25 g, 42%). ^{1}H NMR (D_2O): δ 8.38 (1H, d, *J* = 8.3), 8.18−8.17 (2H, m), 7.86 (1H, t, *J* = 7.4), 7.59 (1H, d, *J* = 8.2), 7.54−7.48 (2H, m), 6.93−6.88 (2H, m), 6.83−6.78 (3H, m), 4.42 (2H, t, *J* = 6.3), 3.63−3.60 (4H, m), 3.54−3.50 (2H, m), 2.80 (3H, s).

Compounds **6a−e** and **6g** were synthesized from **5a−e** and **5g** using a common procedure. Compound **5g** was also used to synthesize **6f**. Representative synthetic procedures are given for **6c** and **6f**.

9-(2-Methylaminoethylamino)acridine-4-carboxylic Acid [2-(3-Phenylureido)ethyl]amide, 6c. A mixture of 1.75 g (3.31 mmol) of **5c** and 100 mL of 2 M NH_4OH was stirred for 15 min and then extracted with 5 × 30 mL of $CHCl_3$. The combined extracts were washed with 2 × 50 mL of water and dried over anhydrous Na_2SO_4. Removal of the solvent under reduced pressure gave **6c** as a yellow solid, which was dried in a vacuum at 60 °C (yield 1.0 g, 66%). ^{1}H NMR ($CDCl_3$): δ 12.86 (1H, br s), 8.67 (1H, d, *J* = 6.8), 8.16−8.11 (2H, m), 7.93 (1H, d, *J* = 8.7), 7.64−7.59 (2H, m), 7.43−7.41 (2H, m), 7.35 (1H, t, *J* = 7.7), 7.24−7.16 (4H, m), 6.96 (1H, t, *J* = 7.4), 6.28 (1H, br s), 3.87 (2H, t, *J* = 5.6), 3.82−3.76 (2H, m), 3.67−3.62 (2H, m), 2.93 (2H, t, *J* = 5.6), 2.54 (3H, s).

9-(2-Methylaminoethylamino)acridine-4-carboxylic Acid (2-Hydroxyethyl)amide, 6f. A mixture of 2.650 g (5.845 mmol) of acetic acid 2{[9-(2-methylaminoethylamino)acridine-4-carbonyl]-amino}ethyl ester trihydrochloride (**5g**) and 4.8 g (35 mmol) of K_2CO_3 in 50 mL of $MeOH/H_2O$ (1:25 v/v) was stirred at room temperature for 2 h. The solvent was partially removed by rotary evaporation, and the product was extracted into $CHCl_3$. The organic layer was dried over anhydrous Na_2SO_4, filtered, and evaporated to dryness to give bright orange crystals of **6f** (1.90 g, 96%). [1]H

NMR (DMSO-d_6): δ 12.5 (1H, br s), 8.63 (1H, d, *J* = 6.8), 8.55 (1H, d, *J* = 8.6), 8.41 (1H, d, *J* = 8.8), 8.0 (1H, d, *J* = 8.4), 7.7 (1H, t, *J* = 7.6), 7.48−7.40 (2H, m), 4.99 (1H, br s), 3.93 (2H, t, *J* = 6.2), 3.73−3.68 (2H, m), 3.60−3.55 (2H, m), 2.87 (2H, t, *J* = 6.3), 2.30 (3H, s).

Compounds **7a−g** were synthesized using a common procedure. A typical synthetic procedure is described below for **7c**.

9-[2-(1,3-Dimethylthioureido)ethylamino]acridine-4-carboxylic Acid [2-(3-Phenylureido)ethyl]amide, 7c. To 1.0 g (2.19 mmol) of **6c** in 25 mL of dry ethanol was added 0.203 g (2.78 mmol) of CH_3NCS in 2 mL of dry ethanol and the mixture was refluxed for 8 h. The solvent was evaporated to dryness, and the residue was recrystallized from MeOH to give golden-yellow needles of compound **7c** (0.700 g, 60%). ^{1}H NMR (MeOH-d_4): δ 8.78 (1H, d, *J* = 8.3), 8.61 (1H, d, *J* = 8.5), 8.37 (1H, d, *J* = 7.3), 7.92 (1H, t, *J* = 7.5), 7.76 (1H, d, *J* = 8.5), 7.55−7.52 (2H, m), 7.21 (2H, d, *J* = 8.0), 7.09 (2H, t, *J* = 7.7), 6.87 (1H, t, *J* = 7.3), 4.52 (2H, t, *J* = 4.7), 4.43 (2H, t, *J* = 4.7), 3.64 (2H, t, *J* = 5.6), 3.54 (2H, t, *J* = 6.0), 3.10 (3H, s), 3.04 (3H, s).

The nitrate salts **8a−g** were generated by adding 1 M HNO_3 (1 or 2 equiv) to the methanolic solutions of the corresponding free bases, **7a−g**. The compounds were precipitated with EtOAc and recrystallized from a mixture of MeOH and EtOAc.

9-[2-(1,3-Dimethylthioureido)ethylamino]acridine-4-carboxylic Acid [2-(3-Ethylureido)ethyl]amide Hydronitrate (8a). Yield: 0.290 g (51%). ^{1}H NMR (MeOH-d_4): δ 8.82 (1H, d, *J* = 8.6, H1), 8.66 (1H, d, *J* = 8.6, H8), 8.38 (1H, d, *J* = 7.3, H3), 7.98 (1H, t, *J* = 7.6, H6), 7.88 (1H, d, *J* = 8.5, H5), 7.60−7.56 (2H, m, H7/H2), 4.53 (2H, t, *J* = 5.1, CH_2 in thiourea linkage), 4.46 (2H, t, CH_2 in thiourea linkage), 3.57 (2H, t, *J* = 5.8, CH_2 in amide residue), 3.46 (2H, t, *J* = 5.8, CH_2 in amide residue), 3.12 (2H, q, *J* = 7.2, C*H$_2$*CH_3), 3.09 (3H, s, CH_3), 3.03 (3H, s, CH_3), 1.05 (3H, t, *J* = 7.2, CH_2C*H$_3$*). ^{13}C{H} NMR (MeOH-d_4): δ 184.3, 169.5, 161.5, 135.6, 53.5, 50.8, 42.3, 40.2, 36.7, 35.9, 33.5, 15.7. (The LC−MS profile and ^{1}H NMR spectrum of **8a** and combustion data for the free base precursor, **7a**, are given as the Supporting Information.)

9-[2-(1,3-Dimethylthioureido)ethylamino]acridine-4-carboxylic Acid [4-(3-Ethylureido)butyl]amide Hydronitrate (8b). Yield: 0.235 g (42%). ^{1}H NMR (MeOH-d_4): δ 8.82 (1H, d, *J* = 8.5, H1), 8.65 (1H, d, *J* = 8.6, H8), 8.40 (1H, d, *J* = 7.3, H3), 7.97 (1H, t, *J* = 7.6, H6), 7.82 (1H, d, *J* = 8.4, H5), 7.58−7.55 (2H, m, H2/H7), 4.53 (2H, t, *J* = 4.8, CH_2 in thiourea linkage), 4.46 (2H, t, *J* = 4.7, CH_2 in thiourea linkage), 3.52 (2H, t, *J* = 7.0, CH_2 in amide residue), 3.20 (2H, t, *J* = 7.0, CH_2 in amide residue), 3.13 (2H, q, *J* = 7.2, C*H$_2$*CH_3), 3.10 (3H, s, CH_3), 3.03 (3H, s, CH_3), 1.76−1.70 (2H, m, CH_2 in amide linkage), 1.64−1.59 (2H, m, CH_2 in amide linkage), 1.08 (3H, t, *J* = 7.2, CH_2C*H$_3$*). ^{13}C{H} NMR (MeOH-d_4): δ 184.3, 169.2, 161.3, 160.3, 137.0, 135.6, 120.4, 120.4, 53.5, 50.79, 40.8, 40.7, 36.8, 35.9, 33.5, 29.0, 27.6, 15.8. Anal. ($C_{26}H_{36}N_8O_5S·CH_3OH$) C, H. N: calcd, 18.53; found, 18.12.

9-[2-(1,3-Dimethylthioureido)ethylamino]acridine-4-carboxylic Acid [2-(3-Phenylureido)ethyl]amide Hydronitrate (8c). Yield: 0.172 g (51%). ^{1}H NMR (MeOH-d_4): δ 8.79 (1H, d, *J* = 8.6, H1), 8.63 (1H, d, *J* = 8.7, H8), 8.38 (1H, d, *J* = 7.4, H3), 7.94 (1H, t, *J* = 7.7, H6), 7.79 (1H, d, *J* = 8.5, H5), 7.57−7.52 (2H, m, H2/H7), 7.21 (2H, d, *J* = 8.1, Ph-*o*-H), 7.09 (2H, t, *J* = 7.9, Ph-*m*-H), 6.87 (1H, t, *J* = 7.4, Ph-*p*-H), 4.55−4.51 (2H, m, CH_2 in thiourea linkage), 4.46−4.42 (2H, m, CH_2 in thiourea linkage), 3.66−3.62 (2H, m, CH_2 in amide residue), 3.56−3.52 (2H, m, CH_2 in amide residue), 3.10 (3H, s, CH_3), 3.03 (3H, s, CH_3). ^{13}C{H} NMR (MeOH-d_4): δ 184.3, 169.8, 160.3, 158.8, 140.7, 136.9, 135.6, 129.7, 123.4, 120.8, 120.4, 120.1, 61.5, 53.5, 50.8, 42.0, 40.3, 36.7, 33.5. Anal. ($C_{28}H_{32}N_8O_5S·0.5H_2O·0.5CH_3COOC_2H_5$) C, N. H: calcd, 5.78; found, 5.34.

9-[2-(1,3-Dimethylthioureido)ethylamino]acridine-4-carboxylic Acid [4-(3-Phenylureido)butyl]amide Hydronitrate (8d). Yield: 0.250 g (45%). ^{1}H NMR (MeOH-d_4): δ 8.82 (1H, d, *J* = 8.6, H1), 8.66 (1H, d, *J* = 8.7, H8), 8.42 (1H, d, *J* = 7.4, H3), 7.97 (1H, t, *J* = 7.7, H6), 7.85 (1H, d, *J* = 8.5, H5), 7.57 (2H, m,

H2/H7), 7.28 (2H, d, $J = 8.5$, Ph-*o*-H), 7.18 (2H, t, $J = 7.9$, Ph-*m*-H), 6.93 (1H, t, $J = 7.3$, Ph-*p*-H), 4.53 (2H, t, $J = 4.8$, CH$_2$ in thiourea linkage), 4.46 (2H, t, $J = 4.9$, CH$_2$ in thiourea linkage), 3.56 (2H, t, $J = 6.9$, CH$_2$ in amide residue), 3.09 (3H, s, CH$_3$), 3.03 (3H, s, CH$_3$), 1.81–1.76 (2H, m, CH$_2$ in amide residue), 1.71–1.65 (2H, m, CH$_2$ in amide linkage). ^{13}C{H} NMR (MeOH-d_4): δ 184.3, 169.2, 160.4, 158.4, 140.9, 137.0, 135.6, 129.7, 123.3, 120.5, 120.4, 120.1, 61.5, 53.5, 50.8, 40.7, 40.4, 36.7, 33.5, 28.7, 27.4, 20.9, 14.5. Anal. (C$_{30}$H$_{36}$N$_8$O$_5$S·0.7CH$_3$COOC$_2$H$_5$) C, H, N.

9-[2-(1,3-Dimethylthioureido)ethylamino]acridine-4-carboxylic Acid (2-Dimethylaminoethyl)amide Hydronitrate (8e). Yield: 0.150 g (47%). ^{1}H NMR (D$_2$O): δ 8.40 (1H, br s, H1), 8.21–8.20 (2H, m, H8/H3), 7.86 (1H, t, $J = 7.6$, H6), 7.60 (1H, d, $J = 8.4$, H5), 7.47–7.41 (2H, m, H7/H2), 4.30–4.28 (2H, m, CH$_2$ in thiourea linkage), 4.22–4.20 (2H, m, CH$_2$ in thiourea linkage), 3.91 (2H, t, $J = 6.2$, CH$_2$ in amide residue), 3.52 (2H, t, $J = 6.2$, CH$_2$ in amide residue), 3.05 (6H, s, N(CH$_3$)$_2$), 2.94 (3H, s, CH$_3$), 2.91 (3H, s, CH$_3$). ^{13}C{H} NMR (MeOH-d_4): δ 184.3, 170.6, 160.4, 137.0, 136.0, 120.4, 119.6, 58.5, 53.5, 50.81, 44.0, 36.7, 36.4, 33.5. Anal. (C$_{23}$H$_{32}$N$_8$O$_7$S·H$_2$O·0.3 CH$_3$COOC$_2$H$_5$) C, H, N.

9-[2-(1,3-Dimethylthioureido)ethylamino]acridine-4-carboxylic Acid (2-Hydroxyethyl)amide Hydronitrate (8f). Yield: 0.280 g (49%). ^{1}H NMR (MeOH-d_4): δ 8.82 (1H, d, $J = 8.6$, H1), 8.65 (1H, d, $J = 8.6$, H8), 8.41 (1H, d, $J = 7.4$, H3), 7.97 (1H, t, $J = 7.7$, H6), 7.84 (1H, d, $J = 8.5$, H5), 7.59–7.55 (2H, m, H7/H2), 4.53 (2H, t, $J = 5.0$, CH$_2$ in thiourea linkage), 4.46 (2H, t, $J = 4.8$, CH$_2$ in thiourea linkage), 3.81 (2H, t, $J = 5.7$, CH$_2$ in amide residue), 3.64 (2H, t, $J = 5.7$, CH$_2$ in amide residue), 3.10 (3H, s, CH$_3$), 3.03 (3H, s, CH$_3$). ^{13}C{H} NMR (MeOH-d_4): δ 184.3, 169.5, 160.3, 137.0, 135.7, 120.7, 120.33, 61.4, 53.5, 50.8, 43.5, 36.7, 33.5. Anal. (C$_{21}$H$_{26}$N$_6$O$_5$S·0.5 CH$_3$COOC$_2$H$_5$) H, N. C: calcd, 53.27; found, 52.81.

Acetic Acid 2-({9-[2-(1,3-Dimethylthioureido)ethylamino]-acridine-4-carbonyl}amino)ethyl Ester Hydronitrate (8g). Yield: 0.300 g (53%). ^{1}H NMR (MeOH-d_4): δ 8.82 (1H, d, $J = 8.6$, H1), 8.64 (1H, d, $J = 8.6$, H8), 8.37 (1H, d, $J = 7.4$, H3), 7.97 (1H, t, $J = 7.7$, H6), 7.84 (1H, d, $J = 8.5$, H5), 7.59–7.55 (2H, m, H2/H7), 4.53 (2H, t, $J = 5.1$, CH$_2$ in thiourea linkage), 4.46 (2H, t, $J = 4.8$, CH$_2$ in thiourea linkage), 4.35 (2H, t, $J = 5.5$, CH$_2$ in amide residue), 3.75 (2H, t, $J = 5.5$, CH$_2$ in amide residue), 3.09 (3H, s, CH$_3$), 3.03 (3H, s, CH$_3$), 2.07 (3H, s, OCH$_3$). ^{13}C{H} NMR (MeOH-d_4): δ 184.3, 172.9, 169.6, 160.4, 137.0, 135.7, 125.4, 123.4, 120.3, 63.8, 53.5, 50.8, 40.3, 36.7, 33.5, 20.8. Anal. (C$_{23}$H$_{28}$N$_6$O$_6$S) C, H, N.

Conjugates **9c–g** were synthesized using a common procedure. A typical procedure is described for **9c** below.

[PtCl(en)(C$_{28}$H$_{32}$N$_7$O$_2$S)](NO$_3$)$_2$, 9c. A mixture of 0.091 g (0.28 mmol) of [PtCl$_2$(en)] and 0.047 g (0.28 mmol) of AgNO$_3$ in 10 mL of anhydrous DMF was stirred at room temperature in the dark for 14 h. The precipitated AgCl was filtered off through a Celite pad, 0.155 g (0.26 mmol) of **8c** was added to the filtrate, and the solution was stirred for 5 h in the dark. The solvent was removed in a vacuum at 30 °C, yielding an oily residue, which was redissolved in hot methanol. The solution was treated with activated carbon and filtered while hot, and the solvent was removed by rotary evaporation. The crude material was redissolved in a minimum amount of methanol and subjected to size exclusion chromatography on a Sephadex LH-20 column using HPLC-grade methanol as the eluent. The collected fractions were subjected to in-line HPLC/mass spectrometry (LC–MS) analysis and the desired fractions were pooled and evaporated to dryness to afford bright yellow microcrystalline complex **9c** (0.120 g, 46%). ^{1}H NMR (D$_2$O): δ 8.41 (1H, d, $J = 8.1$), 8.24 (1H, d, $J = 7.1$), 8.21 (1H, d, $J = 7.4$), 7.89 (1H, t, $J = 7.5$), 7.64 (1H, d, $J = 8.6$), 7.57 (2H, t, $J = 7.2$), 6.96 (2H, br s), 6.86 (3H, br s), 5.20 (br s, NH$_2$, slow H,D exchange), 5.0 (br s, NH$_2$, slow H,D exchange), 4.46 (2H, br s), 4.41 (2H, br s), 3.67 (2H, br s), 3.55 (2H, br s), 3.19 (3H, s), 2.97 (3H, s), 2.60 (4H, br s, broad base due to unresolved Pt-satellites). ESI-MS (MeOH, +ve mode) *m/z*: 819.1 [M − H]$^+$. Anal. (C$_{30}$H$_{40}$N$_{11}$O$_8$-SClPt·3H$_2$O) C, H, N.

[PtCl(en)(C$_{30}$H$_{36}$N$_7$O$_2$S)](NO$_3$)$_2$, 9d. This compound was recrystallized from hot ethanol. Yield: 0.06 g (33%). ^{1}H NMR (D$_2$O): δ 8.45 (1H, d, $J = 8.3$), 8.32 (1H, d, $J = 8.7$), 8.29 (1H, d, $J = 7.4$), 7.97 (1H, t, $J = 7.8$), 7.80 (1H, d, $J = 8.6$), 7.63–7.57 (2H, m), 7.04 (1H, t, $J = 7.7$), 6.93 (1H, t, $J = 7.4$), 6.87 (1H, d, $J = 8.3$), 5.28 (br s, NH$_2$, slow H,D exchange), 5.19 (br s, NH$_2$, slow H,D exchange), 4.47 (4H, br m), 3.55 (2H, t, $J = 6.2$), 3.23 (2H, t, $J = 6.2$), 3.13 (3H, s), 2.91 (3H, s), 2.59 (4H, s, broad base due to unresolved Pt-satellites), 1.82–1.69 (4H, m). ESI-MS (MeOH, +ve mode) *m/z*: 848.2 [M − H]$^+$. Anal. (C$_{32}$H$_{44}$N$_{11}$O$_8$-SClPt·C$_2$H$_5$OH·H$_2$O) C, H, N.

[PtCl(en)(C$_{23}$H$_{32}$N$_6$OS)](NO$_3$)$_3$, 9e. Yield: 0.110 g (43%). ^{1}H NMR (D$_2$O): δ 8.55 (1H, d, $J = 8.5$), 8.40 (1H, d, $J = 8.6$), 8.35 (1H, d, $J = 7.6$), 8.02 (1H, t, $J = 7.4$), 7.88 (1H, d, $J = 8.1$), 7.67–7.65 (2H, m), 5.19 (br s, NH$_2$, slow H,D exchange), 5.01 (br, NH$_2$, slow H,D exchange), 4.53 (4H, br m), 3.94 (2H, t, $J = 6.1$), 3.53 (2H, t, $J = 6.1$), 3.13 (3H, s), 3.05 (6H, s), 2.93 (3H, s), 2.61 (4H, s, broad base due to unresolved Pt-satellites). ESI-MS (MeOH, +ve mode) *m/z*: 729.3 [M-2H]$^+$. Anal. (C$_{25}$H$_{40}$N$_{11}$O$_{10}$-SClPt·2H$_2$O·0.2 CH$_3$COOC$_2$H$_5$) C, H, N.

[PtCl(en)(C$_{21}$H$_{26}$N$_5$O$_2$S)](NO$_3$)$_2$, 9f. Yield: 0.130 g (46%). ^{1}H NMR (D$_2$O): δ 8.46 (1H, d, $J = 8.5$), 8.33 (1H, d, $J = 8.6$), 8.30 (1H, d, $J = 7.4$), 7.99 (1H, t, $J = 7.8$), 7.80 (1H, d, $J = 8.6$), 7.64–7.59 (2H, m), 5.18 (br s, NH$_2$, slow H,D exchange), 5.01 (br s, NH$_2$, slow H,D exchange), 4.48 (4H, br m), 3.88 (2H, t, $J = 5.5$), 3.68 (2H, t, $J = 5.4$), 3.10 (3H, s), 2.87 (3H, s), 2.61 (4H, s, broad base due to unresolved Pt-satellites). ESI-MS (MeOH, +ve mode) *m/z*: 702.2 [M − H]$^+$. Anal. (C$_{23}$H$_{34}$N$_9$O$_8$SClPt) C, H. N: calcd, 15.24; found, 14.78.

[PtCl(en)(C$_{23}$H$_{28}$N$_5$O$_3$S)](NO$_3$)$_2$, 9g. Yield: 0.110 g (51%). ^{1}H NMR (D$_2$O): δ 8.44 (1H, d, $J = 8.5$), 8.30 (1H, d, $J = 8.4$), 8.22 (1H, d, $J = 7.5$), 7.98 (1H, t, $J = 7.8$), 7.77 (1H, d, $J = 8.5$), 7.63–7.58 (2H, m), 5.18 (br s, NH$_2$, slow H,D exchange), 5.01 (br s, NH$_2$, slow H,D exchange), 4.46 (4H, br m), 4.42 (2H, t, $J = 5.2$), 3.79 (2H, t, $J = 5.2$), 3.10 (3H, s), 2.88 (3H, s), 2.61 (4H, s, broad base due to unresolved Pt-satellites), 2.15 (3H, s). ESI-MS (MeOH, +ve mode) *m/z*: 744.2 [M − H]$^+$. Anal. (C$_{25}$H$_{36}$N$_9$O$_9$-SClPt·3H$_2$O) C, H, N.

Molecular Modeling. Molecular mechanics calculations were performed using the AMBER force field in the InsightII/Discover software (version 2000, Accelrys, San Diego, CA). NMR-based energy-minimized models of octamer duplexes containing ACRA-MTU (derivative **1**) were used as starting structures.[14] The structures of derivatives **8b**, **8e**, and **8f** were built with the Biopolymer module and energy-minimized. To produce the drug−DNA complexes, the ACRAMTU molecule was deleted from the starting complexes and replaced with the new threading intercalators by manual docking with the vacant intercalation pocket. The derivatives **8** were inserted regioselectively with the thiourea and 4-carboxamide residues protruding into the minor and major groove, respectively. To induce the proposed hydrogen bonds in the major groove, distance constraints were introduced between the appropriate donor and acceptor atoms using a quadratic harmonic. Initially, these distance constraints were included in the minimizations with force constants of 100 kcal mol^{-1} Å^{-2} and the donor−acceptor distances fixed at $d = 2.5$ Å. During the minimizations, Na$^+$ counterions were used to neutralize the negative charge of the phosphodiester backbone, and solvent was simulated with a distance-dependent dielectric ($\epsilon = 4r_{ij}$). Coulombic and 1−4 parameters were scaled by the common factor of 0.5. The drug−DNA complexes were subjected to steepest descent and conjugate gradient minimization to a final Δrms of 0.01 kcal mol^{-1}Å^{-1} with constraints "on" and to 0.001 kcal mol^{-1}Å^{-1} with contraints "off". Molecular views of the model were generated from *car* files using the DS ViewerPro software (version 6.0, Accelrys, San Diego, CA).

Bioanalytical Assays. (a) Enzymatic Digestion/LC−ESMS Analysis. The stock solutions of **2**, **9e**, and **9f** were prepared in 20 mM Tris buffer (pH 7.1), and the stock solution of **9d** was prepared in DMF. The amount of DMF was less than 1% for **9d** in the final incubation mixtures. The stock solutions were prepared immediately prior to the incubations and if necessary stored at −20 °C. The

calf thymus DNA was purchased from Sigma and its stock solution was made in 20 mM Tris buffer (pH 7.1). The nucleic acid was annealed by slow cooling of the buffered solution from 80 °C to room temperature to ensure that the DNA was in its double-stranded form. DNA concentrations (base pairs, bp) were determined from absorbances at 260 nm using Beer's law with ϵ_{260} (calf thymus) = 12 824 M^{-1} cm^{-1} bp.[48] Millipore water was used for the preparation of all buffers. DNase I and calf intestinal alkaline phosphatase (CIP) were obtained from New England BioLabs, Ipswich, MA, and nuclease P1 (from penicillium citrinium) was from Sigma. Stock solutions of nuclease P1 were prepared in enzyme buffer provided by the vendor. All other chemicals and solvents were purchased from common vendors and used as supplied. HPLC-grade solvents were used in all chromatographic separations. Calf thymus DNA $(2.0 \times 10^{-4}$ M) was incubated with the drugs at a platinum-to-nucleotide ratio (r_i) of 0.05 at 37 °C for 40 h in dark. Incubation of the four drugs was performed in triplicate. The following protocol was used to digest 500-μL samples of the platinum-modified DNA (total incubation time 26 h at 37 °C): (i) 40 μL of 50 mM $MnCl_2$ + 40 units of DNase I (2 h), (ii) 26 units of DNase I (2 h), (iii) 16 units of nuclease P1 (2 h), (iv) 4 units of nuclease P1 (16 h), (v) 20 units of alkaline phosphatase + 20 μL of alkaline phosphatase buffer (2 h), and (vi) 12 units of alkaline phosphatase (2 h). The mixtures were centrifuged at 13 000 rpm for 5 min, and the supernatant was collected. The digested samples were desalted against water for 24 h at room temperature using 100 Da cutoff dialysis membranes and stored at −20 °C. To account for an increase in the sample volume during dialysis, all samples were lyophilized and redissolved in 275 μL of water before (quantitative) LC−MS analysis. The individual adducts were quantified by diode-array UV−visible detection using molar absorptivities for ACRA-MTU and the 4,9-substituted derivatives of 9450 and 9930 M^{-1} cm^{-1}, respectively.

Analytical separation of adducts in enzymatic digestion mixtures was performed using the HPLC module of an Agilent Technologies 1100LS/MSD Trap instrument equipped with a multiwavelength diode-array detector under the following conditions: column, Agilent Zorbax SB-C18 reverse phase 150 × 4.6 mm/5 μm, T = 25 °C; eluents, solvent A, 0.1% formic acid in water, solvent B, 0.1% formic acid in acetonitrile; gradient, 95% A/5% B→65% A/35% B over 0−30 min; flow rate, 0.75 mL/min; injection volume, 20 μL. Elution of Pt−acridine-modified DNA fragments for **2** and **9d**−**f** was monitored at λ_{max} 413 and 422 nm, respectively. Mass spectra were recorded on an Agilent Technologies 1100 LC/MSD ion trap mass spectrometer equipped with an atmospheric pressure electrospray ionization source. The ESMS acquisition parameters were adopted from a published protocol.[11]

(b) Acidic Digestion/LC−ESMS Analysis. The stock solution of **9d** was prepared as described under section a. The oligomer 5′-GCGATATCGC-3′ was synthesized using phosphoramidite chemistry and desalted by Integrated DNA Technologies Inc. (Coralville, IA). The sequence was dissolved in 10 mM Tris buffer (pH 7.2) containing 100 mM NaCl, quantified by UV−visible spectroscopy using ϵ_{260} = 95 600 M^{-1} cm^{-1}, and annealed by slow cooling of the buffered solution from 80 °C to room temperature. Thermal melting curves were recorded of the oligomer to confirm that the sequence was in its double-stranded form at the incubation temperature. All incubations were performed in duplicate at a platinum-to-nucleotide ratio (r_i) of 0.3 at 37 °C for 18 h in the dark. The samples were dialyzed for 48 h against water, treated with formic acid to lower the pH to 2.4, and heated at 60 °C in dark for 12 h. Finally, the digested samples were subjected to in-line LC−MS analysis using the parameters of a published protocol[15] with one exception: the HPLC gradient was modified to 95% A/5% B→81% A/19% B over 0−60 min, at a flow rate of 0.5 mL/min. (Eluents A and B are the same as under section a.)

Cytotoxicity Assay. The cytotoxicity studies were carried out using the Celltiter 96 Aqueous Non-Radioactive Cell Proliferation Assay kit. HL-60 leukemia cells and H460 lung cancer cells were kept in a humidified atmosphere of 5% CO_2/95% air at 37 °C. Cells were plated on 96-well plates with a total of 700 cells/well for

H460 and 27 500 cells/well for HL-60 cells. Stock solutions of **1** and **8a**−**d** were prepared in DMSO while the stock solutions of acridines **8e**−**g** and conjugates **2**, **9c** and **9e**−**g** were prepared in phosphate-buffered saline (PBS). Conjugate **9d** was dissolved in DMF. Prior to the incubations, drug solutions were diluted with media to a final concentration of less than 0.1% in DMSO or DMF. The cells growing in log phase were incubated with appropriate serial dilutions of the drugs in triplicate for 72 h. To each well was added 20 μL of MTS/PMS solution, and the mixtures were allowed to equilibrate for 3 h. The absorbance at 490 nm (none of the derivatives tested absorbs at this wavelength) was recorded using a Precision Microplate Reader (Molecular Devices, Sunnyvale, CA). The reported IC_{50} data were calculated from nonlinear curve fits using a sigmoidal dose−response equation in GraphPad Prism (version 3.02, GraphPad Software Inc., San Diego, CA) and are averages of a minimum of three individual experiments.

Supporting Information Available: Analytical data and LC−MS profiles for selected target compounds and LC−MS results for enzymatic digestion experiments. This material is available free of charge via the Internet at http://pubs.acs.org.

References

(1) Nelson, S. M.; Ferguson, L. R.; Denny, W. A. DNA and the chromosome−Varied targets for chemotherapy. *Cell Chromosome* **2004**, *3*, 2.

(2) Hurley, L. H. DNA and its associated processes as targets for cancer therapy. *Nat. Rev. Cancer* **2002**, *2*, 188−200.

(3) Neidle, S.; Thurston, D. E. Chemical approaches to the discovery and development of cancer therapies. *Nat. Rev. Cancer* **2005**, *5*, 285−296.

(4) Reedijk, J. New clues for platinum antitumor chemistry: Kinetically controlled metal binding to DNA. *Proc. Natl. Acad. Sci. U.S.A.* **2003**, *100*, 3611−3616.

(5) van Zutphen, S.; Reedijk, J. Targeting platinum anti-tumour drugs: Overview of strategies employed to reduce systemic toxicity. *Coord. Chem. Rev.* **2005**, *249*, 2845−2853.

(6) Ackley, M. C.; Barry, C. G.; Mounce, A. M.; Farmer, M. C.; Springer, B. E.; Day, C. S.; Wright, M. W.; Berners-Price, S. J.; Hess, S. M.; Bierbach, U. Structure−activity relationships in platinum-acridi-nylthiourea conjugates: Effect of the thiourea nonleaving group on drug stability, nucleobase affinity, and in vitro cytotoxicity. *J. Biol. Inorg. Chem.* **2004**, *9*, 453−461.

(7) Hess, S. M.; Anderson, J. G.; Bierbach, U. A non-crosslinking platinum−acridine hybrid agent shows enhanced cytotoxicity compared to clinical BCNU and cisplatin in glioblastoma cells. *Bioorg. Med. Chem. Lett.* **2005**, *15*, 443−446.

(8) Hess, S. M.; Mounce, A. M.; Sequeira, R. C.; Augustus, T. M.; Ackley, M. C.; Bierbach, U. Platinum−acridinylthiourea conjugates show cell line-specific cytotoxic enhancement in H460 lung carcinoma cells compared to cisplatin. *Cancer Chemother. Pharmacol.* **2005**, *56*, 337−343.

(9) Martins, E. T.; Baruah, H.; Kramarczyk, J.; Saluta, G.; Day, C. S.; Kucera, G. L.; Bierbach, U. Design, synthesis, and biological activity of a novel non-cisplatin-type platinum-acridine pharmacophore. *J. Med. Chem.* **2001**, *44*, 4492−4496.

(10) Baruah, H.; Rector, C. L.; Monnier, S. M.; Bierbach, U. Mechanism of action of non-cisplatin type DNA-targeted platinum anticancer agents: DNA interactions of novel acridinylthioureas and their platinum conjugates. *Biochem. Pharmacol.* **2002**, *64*, 191−200.

(11) Barry, C. G.; Baruah, H.; Bierbach, U. Unprecedented monofunctional metalation of adenine nucleobase in guanine- and thymine-containing dinucleotide sequences by a cytotoxic platinum−acridine hybrid agent. *J. Am. Chem. Soc.* **2003**, *125*, 9629−9637.

(12) Budiman, M. E.; Alexander, R. W.; Bierbach, U. Unique base-step recognition by a platinum−acridinylthiourea conjugate leads to a DNA damage profile complementary to that of the anticancer drug cisplatin. *Biochemistry* **2004**, *43*, 8560−8567.

(13) Jamieson, E. R.; Lippard, S. J. Structure, recognition, and processing of cisplatin−DNA adducts. *Chem. Rev.* **1999**, *99*, 2467−2498.

(14) Baruah, H.; Bierbach, U. Unusual intercalation of acridin-9-ylthiourea into the 5′-GA/TC DNA base step from the minor groove: Implications for the covalent DNA adduct profile of a novel platinum-intercalator conjugate. *Nucleic Acids Res.* **2003**, *31*, 4138−4146.

(15) Barry, C. G.; Day, C. S.; Bierbach, U. Duplex-promoted platination of adenine-N3 in the minor groove of DNA: Challenging a longstanding bioinorganic paradigm. *J. Am. Chem. Soc.* **2005**, *127*, 1160−1169.

(16) Budiman, M. E.; Bierbach, U.; Alexander, R. W. DNA minor groove adducts formed by a platinum-acridine conjugate inhibit association of TATA-binding protein with its cognate sequence. *Biochemistry* **2005**, *44*, 11262−11268.

(17) Orphanides, G.; Lagrange, T.; Reinberg, D. The general transcription factors of RNA polymerase II. *Genes Dev.* **1996**, *10*, 2657−2683.

(18) Adams, A.; Guss, J. M.; Collyer, C. A.; Denny, W. A.; Wakelin, L. P. Crystal structure of the topoisomerase II poison 9-amino-[*N*-(2-dimethylamino)ethyl]acridine-4-carboxamide bound to the DNA hexanucleotide d(CGTACG)₂. *Biochemistry* **1999**, *38*, 9221−9233.

(19) Adams, A.; Guss, J. M.; Denny, W. A.; Wakelin, L. P. Crystal structure of 9-amino-N-[2-(4-morpholinyl)ethyl]-4-acridinecarboxamide bound to d(CGTACG)₂: Implications for structure−activity relationships of acridinecarboxamide topoisomerase poisons. *Nucleic Acids Res.* **2002**, *30*, 719−725.

(20) Fan, J. Y.; Ohms, S. J.; Boyd, M.; Denny, W. A. DNA adducts of 9-anilinoacridine mustards: Characterization by NMR. *Chem. Res. Toxicol.* **1999**, *12*, 1166−1172.

(21) Fan, J. Y.; Tercel, M.; Denny, W. A. Synthesis, DNA binding and cytotoxicity of 1-[[omega-(9-acridinyl)amino]alkyl]carbonyl-3-(chloromethyl)-6-hydroxyindolines, a new class of DNA-targeted alkylating agents. *Anticancer Drug Des.* **1997**, *12*, 277−293.

(22) Cheng, A. C.; Chen, W. W.; Fuhrmann, C. N.; Frankel, A. D. Recognition of nucleic acid bases and base-pairs by hydrogen bonding to amino acid side-chains. *J. Mol. Biol.* **2003**, *327*, 781−796.

(23) Atwell, G. J.; Cain, B. F.; Baguley, B. C.; Finlay, G. J.; Denny, W. A. Potential antitumor agents. 43. Synthesis and biological activity of dibasic 9-aminoacridine-4-carboxamides, a new class of antitumor agent. *J. Med. Chem.* **1984**, *27*, 1481−1485.

(24) Kopka, K.; Wagner, S.; Riemann, B.; Law, M. P.; Puke, C.; Luthra, S. K.; Pike, V. W.; Wichter, T.; Schmitz, W.; Schober, O.; Schafers, M. Design of new beta1-selective adrenoceptor ligands as potential radioligands for in vivo imaging. *Bioorg. Med. Chem.* **2003**, *11*, 3513−3527.

(25) Augustus, T. M.; Anderson, J.; Hess, S. M.; Bierbach, U. Bis-(acridinylthiourea)platinum(II) complexes: Synthesis, DNA affinity, and biological activity in glioblastoma cells. *Bioorg. Med. Chem. Lett.* **2003**, *13*, 855−858.

(26) Baruah, H.; Wright, M. W.; Bierbach, U. Solution structural study of a DNA duplex containing the guanine-N7 adduct formed by a cytotoxic platinum−acridine hybrid agent. *Biochemistry* **2005**, *44*, 6059−6070.

(27) Kim, J. S.; Kim, J.; Cepek, K. L.; Sharp, P. A.; Pabo, C. O. Design of TATA box-binding protein/zinc finger fusions for targeted regulation of gene expression. *Proc. Natl. Acad. Sci. U.S.A.* **1997**, *94*, 3616−3620.

(28) Dickinson, L. A.; Gulizia, R. J.; Trauger, J. W.; Baird, E. E.; Mosier, D. E.; Gottesfeld, J. M.; Dervan, P. B. Inhibition of RNA polymerase II transcription in human cells by synthetic DNA-binding ligands. *Proc. Natl. Acad. Sci. U.S.A.* **1998**, *95*, 12890−12895.

(29) Dickinson, L. A.; Trauger, J. W.; Baird, E. E.; Ghazal, P.; Dervan, P. B.; Gottesfeld, J. M. Anti-repression of RNA polymerase II transcription by pyrrole-imidazole polyamides. *Biochemistry* **1999**, *38*, 10801−10807.

(30) Chiang, S. Y.; Welch, J.; Rauscher, F. J., 3rd; Beerman, T. A. Effects of minor groove binding drugs on the interaction of TATA box binding protein and TFIIA with DNA. *Biochemistry* **1994**, *33*, 7033−7040.

(31) Woynarowski, J. M.; Trevino, A. V.; Rodriguez, K. A.; Hardies, S. C.; Benham, C. J. AT-rich islands in genomic DNA as a novel target for AT-specific DNA-reactive antitumor drugs. *J. Biol. Chem.* **2001**, *276*, 40555−40566.

(32) Baruah, H.; Barry, C. G.; Bierbach, U. Platinum−intercalator conjugates: From DNA-targeted cisplatin derivatives to adenine binding complexes as potential modulators of gene regulation. *Curr. Topics Med. Chem.* **2004**, *4*, 1537−1549.

(33) Hansen, M.; Hurley, L. Altromycin-B threads the DNA helix interacting with both the major and the minor grooves to position itself for site-directed alkylation of guanine-N7. *J. Am. Chem. Soc.* **1995**, *117*, 2421−2429.

(34) Hansen, M.; Yun, S.; Hurley, L. Hedamycin intercalates the DNA helix and, through carbohydrate-mediated recognition in the minor-groove, directs N7-alkylation of guanine in the major groove in a sequence-specific manner. *Chem. Biol.* **1995**, *2*, 229−240.

(35) Nakatani, K.; Okamoto, A.; Matsuno, T.; Saito, I. Highly selective DNA alkylation at the 5′ side G of a 5′ GG3′ sequence by an aglycon model of pluramycin antibiotics through preferential intercalation into the GG step. *J. Am. Chem. Soc.* **1998**, *120*, 11219−11225.

(36) Sun, D.; Hansen, M.; Clement, J. J.; Hurley, L. H. Structure of the altromycin B (N7-guanine)−DNA adduct. A proposed prototypic DNA adduct structure for the pluramycin antitumor antibiotics. *Biochemistry* **1993**, *32*, 8068−8074.

(37) Sun, D. Y.; Hansen, M.; Hurley, L. Molecular-basis for the DNA-sequence specificity of the pluramycins−A novel mechanism involving groove interactions transmitted through the helix via intercalation to achieve sequence selectivity at the covalent bonding step. *J. Am. Chem. Soc.* **1995**, *117*, 2430−2440.

(38) Hansen, M.; Lee, S.-J.; Cassady, J. M.; Hurley, L. W. Molecular details of the structure of a psorospermin−DNA covalent/intercalation complex and associated DNA sequence selectivity. *J. Am. Chem. Soc.* **1996**, *118*, 5553−5561.

(39) Heald, R. A.; Dexheimer, T. S.; Vankayalapati, H.; Siddiqui-Jain, A.; Szabo, L. Z.; Gleason-Guzman, M. C.; Hurley, L. H. Conformationally restricted analogues of psorospermin: Design, synthesis, and bioactivity of natural-product-related bisfuranoxanthones. *J. Med. Chem.* **2005**, *48*, 2993−3004.

(40) Kostrhunova, H.; Brabec, V. Conformational analysis of site-specific DNA cross-links of cisplatin−distamycin conjugates. *Biochemistry* **2000**, *39*, 12639−12649.

(41) Loskotova, H.; Brabec, V. DNA interactions of cisplatin tethered to the DNA minor groove binder distamycin. *Eur. J. Biochem.* **1999**, *266*, 392−402.

(42) Fan, J. Y.; Valu, K. K.; Woodgate, P. D.; Baguley, B. C.; Denny, W. A. Aniline mustard analogues of the DNA-intercalating agent amsacrine: DNA interaction and biological activity. *Anticancer Drug Des.* **1997**, *12*, 181−203.

(43) Varadarajan, S.; Shah, D.; Dande, P.; Settles, S.; Chen, F. X.; Fronza, G.; Gold, B. DNA damage and cytotoxicity induced by minor groove binding methyl sulfonate esters. *Biochemistry* **2003**, *42*, 14318−14327.

(44) Ohndorf, U. M.; Rould, M. A.; He, Q.; Pabo, C. O.; Lippard, S. J. Basis for recognition of cisplatin-modified DNA by high-mobility-group proteins. *Nature* **1999**, *399*, 708−712.

(45) Zamble, D. B.; Mikata, Y.; Eng, C. H.; Sandman, K. E.; Lippard, S. J. Testis-specific HMG-domain protein alters the responses of cells to cisplatin. *J. Inorg. Biochem.* **2002**, *91*, 451−462.

(46) Cohen, S. M.; Mikata, Y.; He, Q.; Lippard, S. J. HMG-domain protein recognition of cisplatin 1,2-intrastrand d(GpG) cross-links in purine-rich sequence contexts. *Biochemistry* **2000**, *39*, 11771−11776.

(47) Wakelin, L. P.; Bu, X.; Eleftheriou, A.; Parmar, A.; Hayek, C.; Stewart, B. W. Bisintercalating threading diacridines: Relationships between DNA binding, cytotoxicity, and cell cycle arrest. *J. Med. Chem.* **2003**, *46*, 5790−5802.

(48) Jenkins, T. C. Optical absorbance and fluorescence techniques for measuring DNA drug interactions. In *Drug DNA Interaction Protocols;* Fox, K. R, Ed.; Humana Press: Totowa, NJ, 1997; pp 195−218.